JOURNAL OF MATERIALS SCIENCE **39** (2004) 2099–2106

Oxidation resistance of diffusion coatings formed by pack-codeposition of Al and Si on γ-TiAl

Z. D. XIANG, S. R. ROSE, P. K. DATTA
Advanced Materials Research Institute, School of Engineering and Technology, Northumbria University, Ellison Building, Ellison Place, Newcastle upon Tyne, NE1 8ST, UK
E-mail: z.xiang@unn.ac.uk

Oxidation resistance of the aluminide and silicide diffusion coatings pack-deposited on γ-TiAl were studied in air over the temperature range of 800 and 850°C for up to 4596 h. The oxidation kinetics of the coatings was monitored by intermittent weight gain measurement at room temperature. The XRD and SEM/EDS techniques were used to identify the oxide scales formed during the oxidation process and to assess the thermal stability of the coatings at the oxidising temperatures. It was revealed that the $TiAl_3$ coating underwent preferential Al oxidation to form the Al_2O_3 scale in the early oxidation stage, which resulted in Al depletion and formation of $TiAl_2$ in the subsurface of the coating. The Al depletion could not be sufficiently compensated by Al diffusion from the inner layer of the coating and eventually, in the late oxidation stage, led to the Ti oxidation and formation of the TiO_2 phase in the scale. The preferential Si oxidation was the main oxidation mechanism for the coatings with an outer silicide layer and an inner $TiAl_3$ layer with the formation of SiO_2 as the stable oxide scale. The thermal stability of the coatings over the temperature range up to 850°C was discussed in relation to the high-temperature stability of diffusion couples of different coating layers.

1. Introduction

The intermetallic γ-TiAl alloy has attracted much research and significant development in the past decade in an attempt to increase its operating temperature to 850°C and beyond and hence to fully utilise its potential in critical strength application areas particularly in aerospace and power industries where high specific strength and modulus at high temperatures are needed in order to increase operating efficiency [1–3]. It has been demonstrated that the long-term oxidation and corrosion resistance of γ-TiAl at temperatures above 550°C can be significantly improved by protective coatings or through chemical modification of its surface to induce formation of an alumina scale upon oxidation at high temperatures [4, 5]. Among various coating deposition and surface modification techniques, the pack cementation process is widely used to deposit high temperature oxidation and corrosion resistant coatings on nickel-base superalloys and on low alloy steels [6–9]. It has the distinctive advantages of low cost, high volume production and is applicable for a wide range of shapes and sizes without line-of-sight restrictions. As such, a number of studies have been carried out in recent years to use the pack cementation process to aluminise the surface of γ-TiAl for the formation of a $TiAl_3$ surface layer [10–13], which is capable of forming an Al_2O_3 scale upon oxidation in air. However, it has been a common observation that the $TiAl_3$ layer so formed usually contains large numbers of microcracks running across the whole depth of the coating. These microcracks are formed during cooling from aluminising temperatures as a result of mismatch of thermal expansion coefficients between the coating and the substrate and it has been found difficult to form a $TiAl_3$ layer without these microcracks because of the inherent brittleness of $TiAl_3$ [3]. Modifying the γ-TiAl composition by adding alloying elements such as Cr and Nb to the substrate to increase the toughness of the $TiAl_3$ layer has met with limited success in reducing the microcracking tendency of the $TiAl_3$ layer [10]. Attempts have also been made to pack-deposit silicon to form silicide coatings on γ-TiAl [12]. But, it was found that only a porous coating could be formed, which severely degraded the usefulness of the coating.

Nevertheless, in our previous studies [14], it was demonstrated that with adequate control of pack chemistry and deposition conditions, an aluminide coating consisting of an outer $TiAl_3$ layer and an inner $TiAl_2$ layer with a coherent structure free from microcracking could be formed on γ-TiAl by pack cementation. It was also demonstrated that the pack chemistry could be adjusted to codeposit Al and Si to form diffusion coatings on γ-TiAl using elemental Al and Si powders as the depositing source [14]. This paper reports the results of an experimental study on the oxidation resistance and thermal stability of these coatings in air at temperatures up to 850°C.

2. Features of the pack-deposited coatings

The γ-TiAl substrate used in this study has a nominal composition of Ti-31Al-8.6W (wt%). The experimental conditions and procedures for coating deposition and the detailed characterisations of the deposited coatings have been presented previously [14]. Only the key features of these coatings are described below:

2.1. Aluminide coatings

Fig. 1 shows a cross-sectional SEM image and a surface XRD spectrum for this type of coatings, which are designated as TAA. They were deposited at 1000°C for 6 h using packs containing powders of Al, $AlCl_3$ and Al_2O_3. The microstructure of these coatings consists of an outer Al rich $TiAl_3$ layer and an inner Al rich $TiAl_2$ layer with a thickness ratio of $TiAl_3$ to $TiAl_2$ close to one [14]. There also exists a composition gradient at the boundaries of different layers, which provided an essential thermal expansion coefficient transition for maintaining the integrity of the coatings during cooling from the deposition temperature. The total thickness of the coatings is about 36 μm, but this can vary to up to 55 μm depending on the amounts of Al and activator ($AlCl_3$) used in the deposition process. The amount of Al added in the packs should be 4 wt% or less for depositing a coating free of microcracks.

2.2. Silicide/aluminide coatings codeposited at 1100°C

Fig. 2 presents a cross-sectional SEM image and a surface XRD spectrum for this type of coatings, which are designated as TAS. They were deposited at 1100°C for 8 h by a single pack cementation step using packs containing powders of Si, Al, $AlCl_3$ and Al_2O_3. These coatings have a two-layer structure consisting of an outer silicide layer of approximately 8 μm and an inner $TiAl_3$ layer of approximately 23 μm [14]. There is also a transition layer or diffusion zone at the boundary between the inner $TiAl_3$ layer and the substrate, which ensured the integrity of the coating during cooling from the

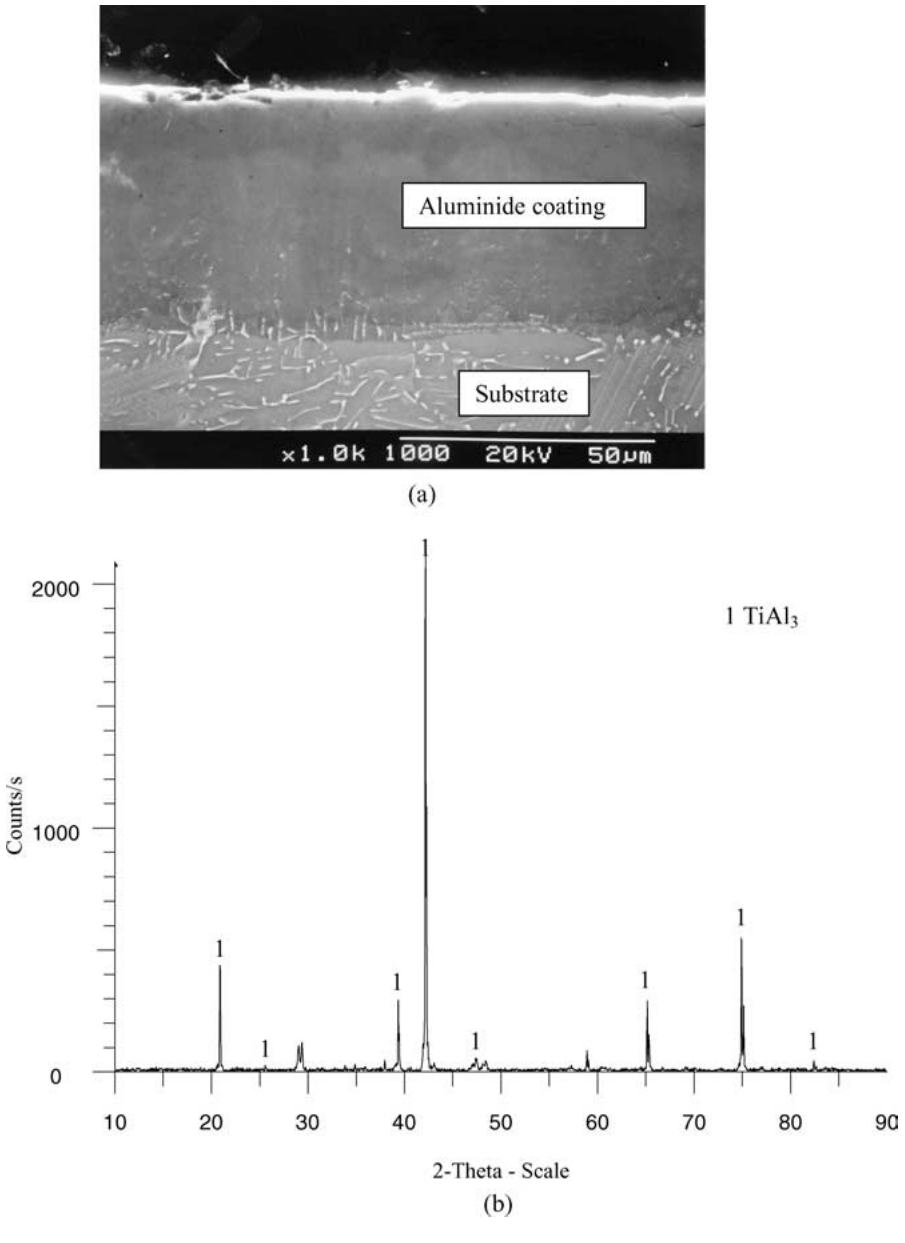

Figure 1 The cross-sectional SEM image and XRD spectrum of as-coated TAA coating.

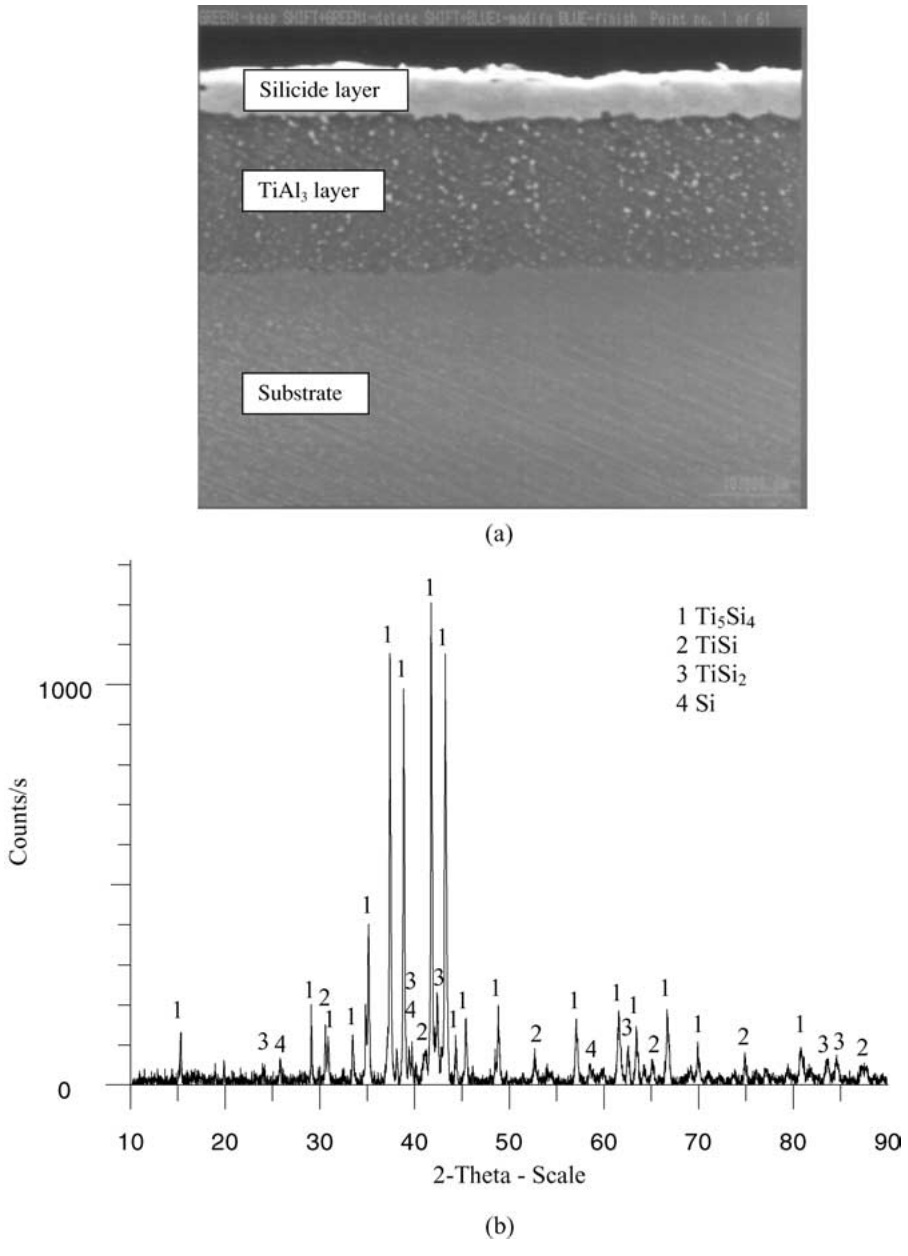

Figure 2 The cross-sectional SEM image and XRD spectrum of as-coated TAS coating.

deposition temperature. The major phase in the outer silicide layer is Ti_5Si_4 and the minor phases include TiSi, $TiSi_2$ and Si.

3. Experimental details

The oxidation tests were conducted in an open-ended tube furnace with air as the oxidising atmosphere. The samples were oxidised at 850°C for up to 240 h and at 800°C for more than 4500 h to evaluate their short-term and long-term oxidation resistance at respective temperatures. The oxidation process was monitored by intermittent weight measurement of the specimens at room temperature. The specimens were rapidly taken out of the furnace to cool at room temperature for a weight measurement and then back into the furnace to continue the oxidation tests. X-ray diffraction (XRD) (Siemens Diffraktometer 5000, Cu K_α source radiation) and scanning electron microscope (SEM) equipped with energy dispersive spectroscopy (EDS) and back-scattered electron imaging (Hitachi S-2400) were used to identify the oxide scales and to assess the thermal stability of the coatings. The coating thickness was estimated from the depth profiles of element concentrations in the coating layer measured by the EDS.

4. Results and discussions

4.1. Short-term oxidation studies at 850°C

Fig. 3 presents the oxidation kinetics data at 850°C for the substrate and coatings. The weight loss of the substrate occurring at about 170 h oxidation was due to disintegration and spallation of the oxidised surface layer. In contrast, all the coatings maintained their integrity with no detectable sign of spallation or microcracking, demonstrating good oxidation resistance needed for protecting the substrate. It is evident that the TAS coating was more oxidation resistant than the TAA coating.

Fig. 4 shows the XRD spectrum of the TAA coating at the end of 240 h oxidation test. It is clear that Al_2O_3 is the only oxide present and no TiO_2 could be

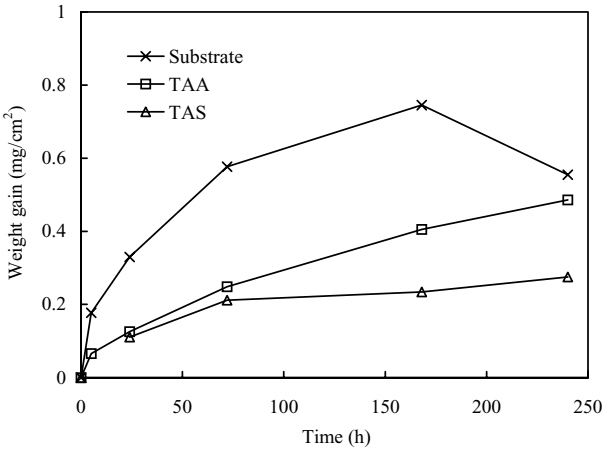

Figure 3 Interrupted oxidation data at 850°C.

detected in the scale. Because the Al_2O_3 scale is very thin (~4 μm), the diffraction pattern of the coating just beneath the scale are also present in the spectrum with peaks of high intensity attributable to $TiAl_3$ and $TiAl_2$. The $TiAl_2$ phase was not present in the original surface layer of the coating, but formed in the subsurface of the coating during the oxidation process. The formation of this phase was caused by Al depletion as a result of preferential Al oxidation in the $TiAl_3$ coating. The Al depletion in the subsurface could not be fully compensated by the outward Al diffusion from the inner surface layer at the oxidation temperature. It is thus reasonable to suggest that the oxidation of $TiAl_3$ at 850°C during the 240 h test period was primarily followed by

$$TiAl_3 + 3/4O_2 = TiAl_2 + 1/2Al_2O_3 \qquad (1)$$

This observation is in close agreement with the predicted oxidation mechanism [15, 16].

Fig. 5 shows the XRD spectrum of the TAS coating taken at the end of 240 h oxidation. Because the scale formed was very thin (~ only 1 μm), it is extremely difficult to resolve the weak diffraction peaks of the oxides from the strong ones of the coating in the subsurface. The major phase that can be convincingly detected is Ti_5Si_3 with the $TiSi_2$ and TiSi as the minor phases. This can be compared with the phase constituents in the original coating before the oxidation test, which had the Ti_5Si_4 as the major phase and the $TiSi_2$ and TiSi as the minor phases (Fig. 2b). Thus, at the end of 250 h oxidation, the Ti_5Si_4 phase was totally converted to Ti_5Si_3, at least in the subsurface of TAS coating. This indicates a preferential Si oxidation mechanism according to

$$Ti_5Si_4 + O_2 = Ti_5Si_3 + SiO_2 \qquad (2)$$

which suggests that the scale formed would be SiO_2. As will be presented later, this agrees well with the results of EDS analysis, which indicated that the scale formed consisted mostly of SiO_2. The thermodynamic calculations also predicted that preferential Si oxidation to form SiO_2 in the Ti_5Si_3–$TiSi_2$ phase range is possible over the temperature range of 700 to 1000°C [15].

Fig. 6 shows the cross-section SEM image and element concentration profiles in the coating layer measured by EDS for the TAA coating at the end of 240 h oxidation test. It can be seen that a continuous scale with a thickness of about 4 μm was formed on the coating surface. The EDS data showed that Al is the only major metal element present in the scale, confirming that the scale formed is Al_2O_3, which is in agreement with the XRD analysis. The coating maintained its integrity with no observable spallation and microcracking. But, it is evident from the EDS data in Fig. 7 that the coating thickness was increased from about 36 μm before the oxidation (Fig. 1) to about 66 μm at the end of 240 h oxidation test. As described previously (Section 2.1), the original coating had an outer Al rich $TiAl_3$ layer and an inner Al rich $TiAl_2$ layer. The increase in total coating thickness after the oxidation test was no doubt caused by further inward Al diffusion from these layers at the oxidation temperature. This tendency of further inward Al diffusion is potentially a

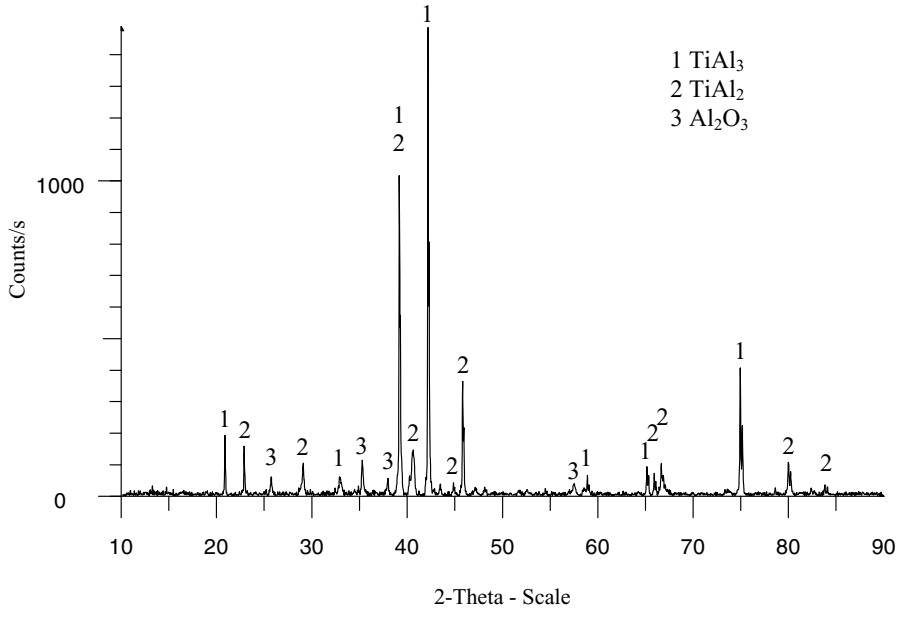

Figure 4 XRD spectrum of the TAA coating after 240 h oxidation in air at 850°C.

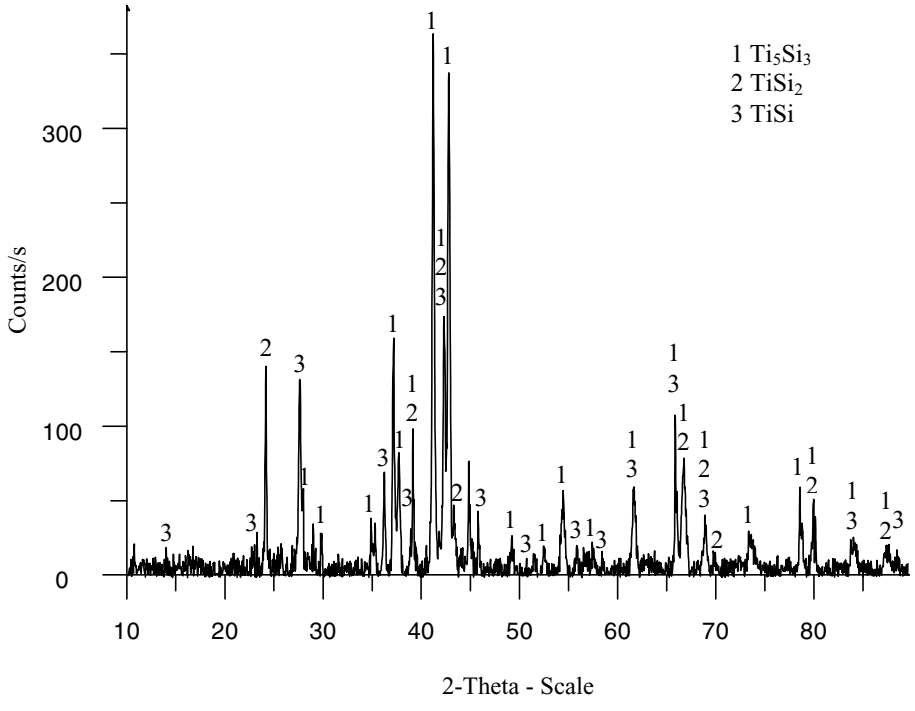

Figure 5 XRD spectrum of the TAS coating after 240 h oxidation in air at 850°C.

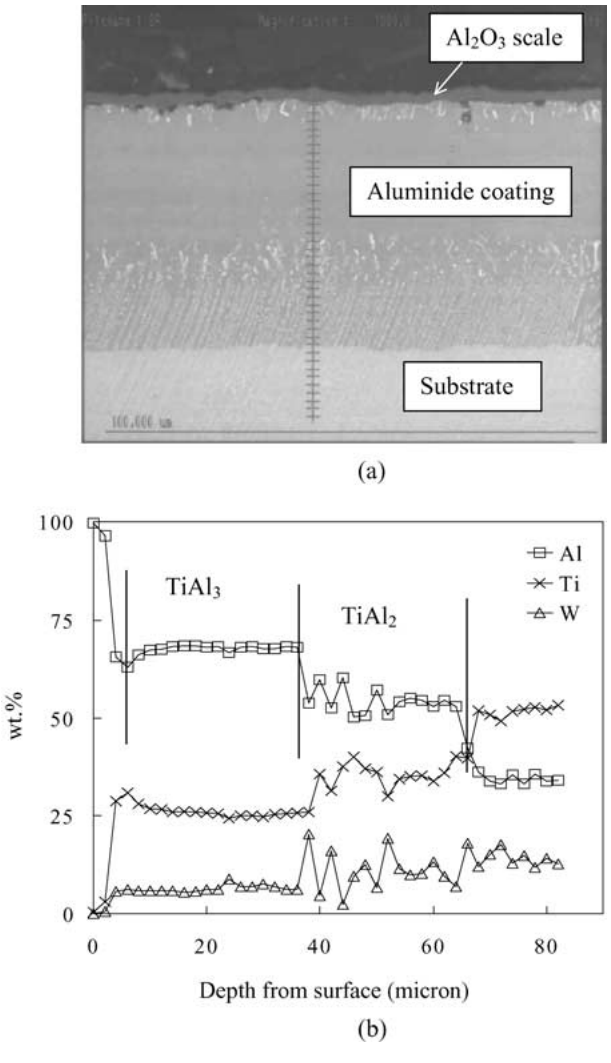

Figure 6 Cross-sectional SEM image and element concentration profiles in the TAA coating layer after intermittent oxidation in air for 240 h at 850°C.

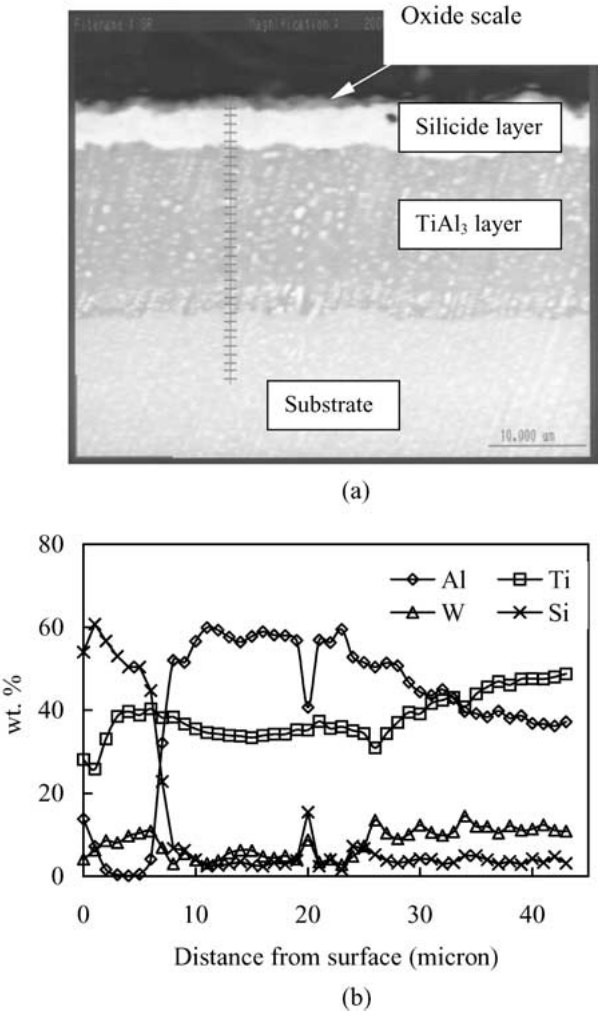

Figure 7 Cross sectional SEM image and element concentration profiles in the TAS coating layer after oxidation test in air at 850°C for 240 h.

significant factor that can affect the long-term thermal stability and hence the effective working life of the coating. However, the results of Loo and Reicks' diffusion studies [17] seemed to indicate that, at temperatures below 1000°C, the diffusion couples such as $TiAl/TiAl_2$ and $TiAl_2/TiAl_3$, which have only one phase boundary, would be stable. In the absence of diffusion data for the complex phase couple of $TiAl_3/TiAl_2/TiAl$, which correspond to the structure of the coating produced in this study, it is not possible at this stage to accurately assess the thermal stability of the coating at the oxidation temperature of 850°C. More detailed diffusion studies are needed to clarify whether the observed increase in total coating thickness was reached at the end or at an intermediate stage of the 240 h oxidation test.

However, it is of major significance to note that despite an increase in the overall coating thickness after the oxidation tests, the thickness ratio of the outer $TiAl_3$ layer to the inner $TiAl_2$ layer remained almost the same as that before the oxidation tests, which was close to one [14]. This indicates a uniform growth rate for both $TiAl_3$ and $TiAl_2$ phase layers in the coating during the oxidation process, which seems to imply that the diffusion rate of Al in the $TiAl_3$, $TiAl_2$ and TiAl phases was uniform at the oxidation test temperature of 850°C.

Fig. 7 presents the cross-sectional SEM image and element concentration profiles in the coating layer measured by EDS for the TAS coating after the 240 h oxidation. Again, it can be seen that the coating maintained its excellent integrity with no measurable sign of spallation or microcracking. An oxide scale with a thickness of about 1 μm on the coating surface is clearly visible in the SEM image. The EDS data showed that the top surface of the oxide scale contained approximately 14 wt% Al, 28 wt% Ti, and 54 wt% Si. If all these elements were assumed to be present in the oxide form, it can be estimated that the molar ratio of Al_2O_3:TiO_2:SiO_2 in the surface of the scale would be approximately 1:2:7. Thus, the scale is exceedingly rich in silica. This is consistent with the XRD analysis, which revealed that the preferential oxidation of Si in Ti_5Si_4 controls the oxidation mechanism at the testing temperature. Fig. 7 also shows that despite the formation of a thin layer of oxide scale, the overall coating structure remained largely unaffected by the oxidation process, consisting of a top silicide layer with a thickness of about 6 μm and an inner aluminide layer with a thickness of about 21 μm. Therefore, the total thickness of the coating at the end of 240 h oxidation test was about 27 μm. This compares favourably with 31 μm measured for the as-coated specimen (Section 2.2). As the two series of specimens were prepared using packs of two different batches, the difference between the two can be attributed to the batch-to-batch variations. More significantly, as can be easily estimated from the element concentration profiles, the molar ratio of Al to Ti in the inner aluminide layer of the coating at the end of oxidation test was approximately 3, suggesting a $TiAl_3$ phase, which is the same as that for the original coating. Therefore, the overall microstructure of the TAS coating remained essentially unchanged with no significant inward Al diffusion taking place at the interface between the inner $TiAl_3$ layer of the TAS coating and the substrate during the oxidation process. Therefore, it may be concluded that the TAS coating is thermally stable at temperatures up to 850°C.

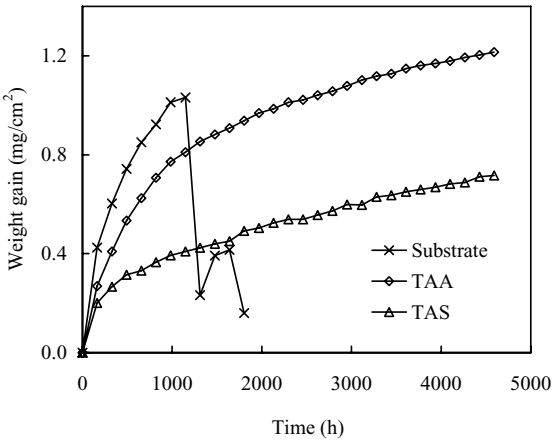

Figure 8 Interrupted oxidation data at 800°C.

4.2. Long-term oxidation resistance at 800°C

The long-term oxidation resistance of the coatings at 800°C was tested in the same way as described in the previous section. Fig. 8 presents the weight gain data of the substrate and coatings as a function of time for the period of more than 4500 h. For the substrate, disintegration and spallation of the scale occurred after approximately 1150 h oxidation as evidenced by the sudden weight loss. The accumulated weight gain was 1.0 $mg \cdot cm^{-2}$. To reach the same level of weight gain, the TAA coating needed more than 2400 h oxidation. More importantly, the TAA coating showed no sign of scale spallation or microcracking during the entire oxidation period of more than 4500 h during which its accumulated weight gain was 1.2 $mg \cdot cm^{-2}$, suggesting that it can effectively enhance the oxidation resistance of the substrate through the formation of a more stable and adherent oxide scale. The TAS coating was even more oxidation resistant. At the end of more than 4500 h oxidation, the weight gain of the TAS coating was only about 0.7 $mg \cdot cm^{-2}$ with no detectable sign of spallation or microcracking.

Fig. 9 presents the XRD spectrum of the TAA coating taken after oxidising at 800°C for 2788 h. It shows similar features to the XRD spectrum taken after oxidation at 850°C for 240 h (Fig. 4). The $TiAl_2$ and Al_2O_3 phases detected in both cases are the oxidation products of $TiAl_3$ through a mechanism described by Equation 1. The key difference between the two spectra is the presence of TiO_2 in the scale formed at 800°C after 2788 h oxidation, which was not present in the scale formed at 850°C after 240 h oxidation. The implication of this observation is that the initial oxidation process of the TAA coating only involved the preferential Al oxidation. After sufficiently long oxidation period, oxidation of Ti in the TAA coating started to occur as a consequence of the continued Al depletion in the subsurface that could not be sufficiently compensated by the Al diffusion from the inner surface layers of the TAA

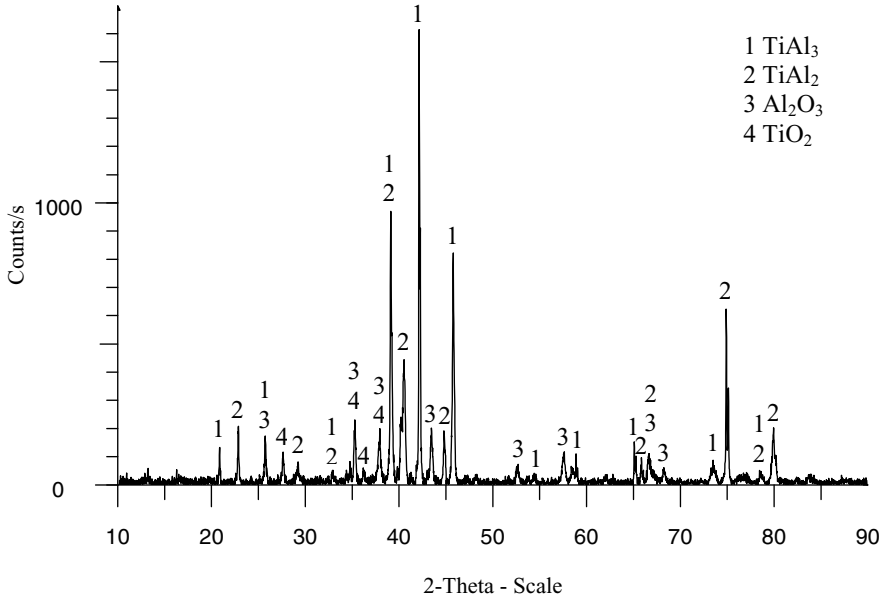

Figure 9 XRD spectrum of the TAA coating after oxidation in air at 800°C for 2788 h.

coating. No TiAl and Ti_3Al phases could be detected by XRD. Thus, the possible oxidation steps leading to the formation of TiO_2 as a consequence of the Al depletion in the subsurface could be

$$TiAl_2 + 3/4O_2 = TiAl + 1/2Al_2O_3 \quad (3)$$

$$TiAl + O_2 = TiO_2 + Al \quad (4)$$

$$Al + TiAl = TiAl_2 \quad (5)$$

Fig. 10 presents the cross-sectional SEM image and element concentration profiles measured by EDS in the TAA coating layer for the same specimen as the one on which surface the XRD spectrum of Fig. 9 was taken. The Al depletion zone in the subsurface between the Al_2O_3 scale and the outer $TiAl_3$ layer is clearly recognisable from the Al and Ti concentration profiles.

The XRD spectrum of the TAS coating after 2788 h oxidation at 800°C was also taken, but it showed no significantly different features from those of the spectrum taken after 240 h oxidation at 850°C (Fig. 5). The phases detected included mainly Ti_5Si_3, TiSi and $TiSi_2$. Again, due to the thin nature of the scale formed (~3 μm), it is not possible to convincingly resolve the weak diffraction peaks of the oxide phases in the scale from those of the coating in the subsurface. Nevertheless, thermodynamic analysis suggested that the oxidation tendency of the silicide phases at 800°C would not be different from that at 850°C [15, 16]. Thus, as at 850°C, the preferential Si oxidation leading to the formation of mainly the SiO_2 scale was also the main oxidation process of the TAS coating at 800°C.

Fig. 11 presents the cross-sectional SEM image of the TAS coating after 2788 h oxidation at 800°C. It can be seen that, except a thicker oxide scale (~3 μm), it reveals basically the same features as in the same coating after 240 h oxidation at 850°C (Fig. 7). The element concentration profiles in the coating layer measured using EDS were also essentially of the same features as shown in Fig. 7 and hence are omitted here. These observations confirmed that the TAS coating is thermally stable at 800°C, consistent with the observations at 850°C.

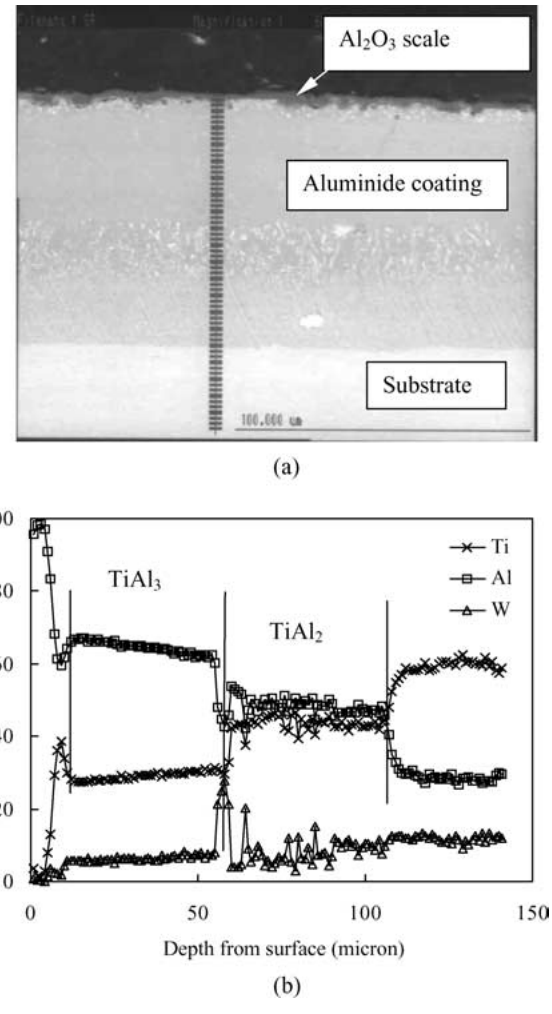

Figure 10 Cross-sectional SEM image and element concentration profiles in the TAA coating layer after intermittent oxidation in air at 800°C for 2788 h.

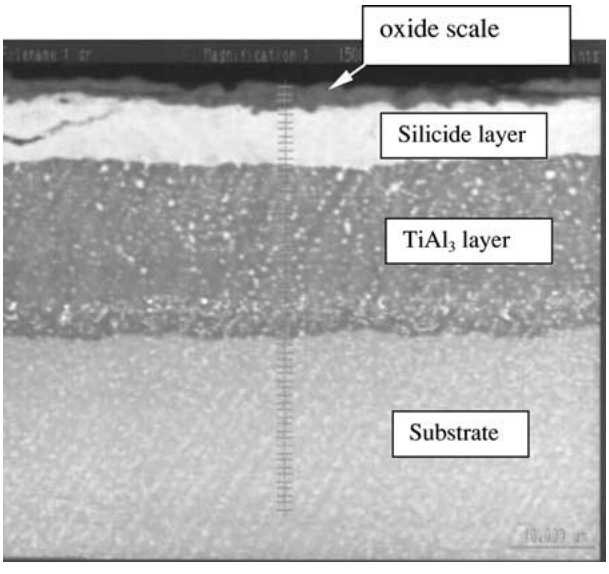

Figure 11 Cross-sectional SEM image of the TAS coating layer after 2788 h oxidation in air at 800°C.

5. Conclusions

For the coatings consisting of an outer $TiAl_3$ layer and an inner $TiAl_2$ layer, the early stage of oxidation in air over the temperature rang up to 850°C was dominated by preferential Al oxidation with the formation of Al_2O_3 as the scale and $TiAl_2$ as a new major phase in the subsurface layer of the coating. Further oxidation eventually led to the Ti oxidation as a result of the continued Al depletion that could not be fully compensated by the Al diffusion from the inner $TiAl_3$ surface layer. While the coatings could enhance the oxidation resistance of γ-TiAl, the thermal stability of these coatings was ultimately determined by the thermal stability of diffusion couple $TiAl_3/TiAl_2/TiAl$ at high temperatures.

For the coatings consisting an outer silicide layer and an inner $TiAl_3$ layer, the oxidation process in air over the temperature range up to 850°C was controlled primarily by the preferential Si oxidation with the formation of SiO_2 as the scale. The oxidation at the early stage involved the conversion of Ti_5Si_4 to Ti_5Si_3. These coatings are thermally stable with no significant diffusions between different layers and can provide an effective protection against oxidation for γ-TiAl over the temperature range studied.

References

1. W. KAYSSER, *Surf. Engng.* **17**(4) (2001) 305.
2. A. RAHMEL, W. J. QUADAKKERS and M. SCHUTZE, *Mater. Corrs.* **46** (1995) 271.
3. M. YAMAGUCHI, *Mater. Sci. Technol.* **8**(4) (1992) 299.
4. Z. TANG, L. NIEWOLAK, V. SHEMET, L. SINGHEISER, W. J. QUADAKKERS, F. WAND, W. WU and A. GIL, *Mater. Sci. Eng.* A **328** (2002) 297.
5. M. P. BRADY, W. J. BRINDLEY, J. L. SMIALEK and I. E. LOCCI, *JOM* **48**(11) (1996) 46.
6. Z. D. XIANG, J. S. BURNELL-GRAY and P. K. DATTA, *J. Mater. Sci.* **36** (2001) 5673.
7. *Idem.*, *Surf. Engng.* **17**(4) (2001) 287.
8. R. MEVREL, C. DURET and R. PICHOIR, *Mater. Sci. Technol.* **2**(3) (1986) 201.
9. S. R. LEVIN and R. M. CAVES, *J. Electrochem. Soc.* **121**(8) (1974) 1051.
10. H. G. JUNG and K. Y. KIM, *Oxid. Met.* **58**(1/2) (2002) 197.
11. C. ZHOU, H. BIN and K. Y. KIM, *Metall. Mater. Trans.* A **31A** (2000) 2391.
12. T. C. MUNRO and B. GLEESON, *ibid.* **27A** (1996) 3761.
13. J. SUBRAHMANYAM, *J. Mater. Sci.* **23** (1988) 1906.
14. Z. D. XIANG, S. R. ROSE, J. S. BURNELL-GRAY and P. K. DATTA, *ibid.* **38** (2002) 19.
15. A. RAHMEL and P. J. SPENCER, *Oxid. Met.* **35**(1/2) (1991) 53.
16. K. L. LUTHRA, *ibid.* **36** (1991) 475.
17. F. J. J. LOO and G. D. RIECK, *ACTA Metall.* **21** (1973) 73.

Received 12 December 2002
and accepted 5 November 2003